

---

# Hadron production in heavy relativistic systems

ROLF KUIPER<sup>1,2</sup> and GEORG WOLSCHIN<sup>1</sup>

<sup>1</sup> *Institut für Theoretische Physik, Philosophenweg 16, 69120 Heidelberg, Germany*

<sup>2</sup> *now at Max Planck Institute for Astronomy, Königstuhl 17, 69117 Heidelberg, Germany*

PACS 25.75.-q – Relativistic heavy-ion collisions

PACS 24.60.Ky – Fluctuation phenomena

PACS 24.10.Jv – Relativistic models

**Abstract.** – We investigate particle production in heavy-ion collisions at RHIC energies as function of incident energy, and centrality in a three-sources Relativistic Diffusion Model. Pseudorapidity distributions of produced charged hadrons in Au + Au and Cu + Cu collisions at  $\sqrt{s_{NN}} = 19.6$  GeV, 62.4 GeV, 130 GeV and 200 GeV show an almost equilibrated midrapidity source that tends to increase in size towards higher incident energy, and more central collisions. It may indicate quark-gluon plasma formation prior to hadronization.

---

**Introduction.** – The precise calculation and prediction of transverse momentum and rapidity distributions of produced particles is of basic importance in relativistic heavy-ion physics. In this Letter we propose nonequilibrium-statistical methods [1] to investigate analytically the gradual thermalization in rapidity space occurring in the course of particle production at the highest available energies. The approach is tailored to identify the fraction of produced particles in local thermal equilibrium from their pseudorapidity distribution functions in heavy systems, with a focus on Cu + Cu and Au + Au. It may yield indirect evidence for the extent and energy dependence of a locally equilibrated parton plasma.

There exist other theoretical approaches that allow to compute rapidity distribution functions for produced particles, albeit with less precision. Some of them are based on QCD, such as calculations within the framework of the Parton Saturation Model [2]. Ideal hydrodynamics is well developed in its applications to relativistic collisions, but more realistic dissipative hydrodynamic approaches are still in the early stage of theoretical development [3].

Thermal models are outstanding in their ability to correctly predict particle abundance ratios at midrapidity, or momentum integrated [4, 5]. But since these approaches do not deal with nonequilibrium-statistical effects, one can not expect precise results for distribution functions whenever hadronic or partonic thermalization processes through multiple collisions on an event-by-event basis are important [5]. Within a thermal model, such effects could be simulated to some extent by different values of local temperature and chemical potential when investigating particle production at different rapidities.

Hence, nonequilibrium statistics is the natural choice for a detailed description of the gradual approach to statistical equilibrium in relativistic collisions of heavy systems. Our Relativistic Diffusion Model (RDM) underlines the nonequilibrium-statistical features of high-energy heavy-ion collisions, but it also encompasses kinetic (thermal) equilibrium of the system for times that are sufficiently larger than the relaxation times of the relevant variables.

It is of particular interest in relativistic collisions of heavy systems to determine the fraction of produced particles that attains - or comes very close to - statistical equilibrium with respect to a specific macroscopic variable, such as rapidity. In the three-sources RDM, these are the particles produced in the midrapidity source. Hence we analyze Au + Au and Cu + Cu pseudorapidity distributions of produced particles at RHIC energies from  $\sqrt{s_{NN}}=19.6 - 200$  GeV corresponding to beam rapidities  $y_{max}=3.04 - 5.36$ . We determine the transport coefficients and numbers of produced particles in the midrapidity source as functions of the incident energies, and centralities.

**Relativistic Diffusion Model.** – In the Relativistic Diffusion Model, the rapidity distribution of produced particles at RHIC energies emerges from an incoherent superposition of the beam-like components that are broadened in rapidity space through diffusion processes, and a near-equilibrium (thermal) component at midrapidity that may indicate local quark-gluon plasma (QGP) formation.

The time evolution of the distribution functions is governed by a Fokker-Planck equation (FPE) in rapidity space [1, 6–10]

$$\frac{\partial}{\partial t}[R(y, t)]^\mu = -\frac{\partial}{\partial y}\left[J(y)[R(y, t)]^\mu\right] + D_y \frac{\partial^2}{\partial y^2}[R(y, t)]^\nu \quad (1)$$

with the rapidity  $y = 0.5 \cdot \ln((E + p)/(E - p))$ . The rapidity diffusion coefficient  $D_y$  that contains the microscopic physics accounts for the broadening of the rapidity distributions. The drift  $J(y)$  determines the shift of the mean rapidities towards the central value, and linear and nonlinear forms have been discussed.

Here we use  $\mu = 1$  (due to norm conservation) and  $\nu = 2 - q$  with the nonextensivity parameter [11]  $q = 1$  corresponding to the standard FPE, and a linear drift function

$$J(y) = (y_{eq} - y)/\tau_y \quad (2)$$

with the rapidity relaxation time  $\tau_y$ , and the equilibrium value  $y_{eq}$  of the rapidity [1, 10]. This is the so-called Uhlenbeck-Ornstein [12] process, applied to the relativistic invariant rapidity for the three components  $R_k(y, t)$  ( $k=1,2,3$ ) of the distribution function in rapidity space [1, 6, 9, 13]

$$\frac{\partial}{\partial t}R_k(y, t) = \frac{1}{\tau_y} \frac{\partial}{\partial y}\left[(y - y_{eq}) \cdot R_k(y, t)\right] + D_y^k \frac{\partial^2}{\partial y^2}R_k(y, t). \quad (3)$$

Since the equation is linear, a superposition of the distribution functions [1, 6] using the initial conditions  $R_{1,2}(y, t = 0) = \delta(y \pm y_{max})$  with the absolute value of the beam rapidities  $y_{max}$ , and  $R_3(y, t = 0) = \delta(y - y_{eq})$  yields the exact solution. In the solution, the mean values and variances are obtained analytically from the moments equations. The equilibrium value  $y_{eq}$  is calculated at each centrality from energy- and momentum conservation among the participants. For symmetric systems it is  $y_{eq} = 0$  independently of centrality, but its deviation from zero is important for precise calculations of rapidity distributions in case of asymmetric systems [10].

**Pseudorapidity distributions.** – If particle identification is not available, one has to convert the results to pseudorapidity,  $\eta = -\ln[\tan(\theta/2)]$  with the scattering angle  $\theta$ . The conversion from  $y$ - to  $\eta$ - space of the rapidity density

$$\frac{dN}{d\eta} = \frac{p}{E} \frac{dN}{dy} = J(\eta, \langle m \rangle / \langle p_T \rangle) \frac{dN}{dy} \quad (4)$$

Table 1: Produced charged hadrons as functions of centrality in Cu + Cu and Au + Au collisions at  $\sqrt{s_{NN}} = 19.6, 62.4, 130$  and 200 GeV in the Relativistic Diffusion Model. The number of produced charged particles at each centrality is  $N_{ch}^{tot}$ , the percentage of charged particles produced in the thermalized source is  $n_{ch}^{eq}$ . The ratio  $\tau_{int}/\tau_y$  determines how fast the system of produced charged particles equilibrates in rapidity space. The widths of the peripheral sources are  $\Gamma_{1,2}$ , the width of the midrapidity source is  $\Gamma_{eq}$ . The  $\chi^2/d.o.f.$  values with constraints are discussed in the text.

System	$\sigma_{tot}$	$N_{ch}^{tot}$	$n_{ch}^{eq}(\%)$	$\frac{\tau_{int}}{\tau_y}$	$\Gamma_{1,2}$	$\Gamma_{eq}$	$\frac{\chi^2}{d.o.f.}$
Cu+Cu 62.4 GeV	0 - 6%	825	3.2	1.12	3.70	5.16	$\frac{4.7}{49}$
	6 - 15%	681	2.2	1.11	3.70	4.92	$\frac{2.4}{49}$
	15 - 25%	494	1.4	1.09	3.70	4.73	$\frac{1.5}{40}$
	25 - 35%	340	0.9	1.09	3.70	4.57	$\frac{3.0}{40}$
	35 - 45%	230	0.4	1.08	3.70	4.45	$\frac{4.9}{40}$
Cu+Cu 200 GeV	0 - 6%	1474	7.1	1.08	4.03	2.45	$\frac{2.0}{49}$
	6 - 15%	1129	6.2	1.07	4.03	2.40	$\frac{1.0}{49}$
	15 - 25%	791	5.4	1.06	4.03	2.35	$\frac{1.8}{49}$
	25 - 35%	536	4.9	1.05	4.03	2.31	$\frac{3.5}{49}$
	35 - 45%	349	4.3	1.05	4.03	2.28	$\frac{5.7}{49}$
	45 - 55%	216	4.2	1.04	4.03	2.24	$\frac{8.2}{49}$
Au+Au 19.6 GeV	0 - 6%	1691	-	1.23	2.90	-	$\frac{0.7}{28}$
	6 - 15%	1323	-	1.19	2.90	-	$\frac{0.4}{28}$
	15 - 25%	966	-	1.15	2.90	-	$\frac{0.5}{28}$
	25 - 35%	672	-	1.12	2.90	-	$\frac{1.5}{28}$
	35 - 45%	429	-	1.10	2.90	-	$\frac{1.9}{27}$
Au+Au 130 GeV	0 - 6%	4233	13.2	1.02	3.56	2.64	$\frac{3.7}{49}$
	6 - 15%	3318	11.9	1.02	3.56	2.45	$\frac{1.0}{49}$
	15 - 25%	2313	10.9	1.01	3.56	2.28	$\frac{1.3}{41}$
	25 - 35%	1559	10.0	1.01	3.56	2.14	$\frac{3.1}{41}$
	35 - 45%	1005	9.3	1.00	3.56	2.05	$\frac{6.2}{41}$
	45 - 55%	615	8.6	1.00	3.56	1.93	$\frac{9.7}{41}$
Au+Au 200 GeV	0 - 6%	5123	26.3	0.93	3.51	3.20	$\frac{1.1}{49}$
	6 - 15%	3987	24.8	0.93	3.51	3.08	$\frac{0.8}{49}$
	15 - 25%	2827	23.7	0.92	3.51	2.97	$\frac{2.3}{49}$
	25 - 35%	1916	22.7	0.92	3.51	2.90	$\frac{7.9}{49}$
	35 - 45%	1251	21.9	0.92	3.51	2.83	$\frac{11.7}{49}$
	45 - 55%	762	21.1	0.91	3.51	2.76	$\frac{15.4}{49}$

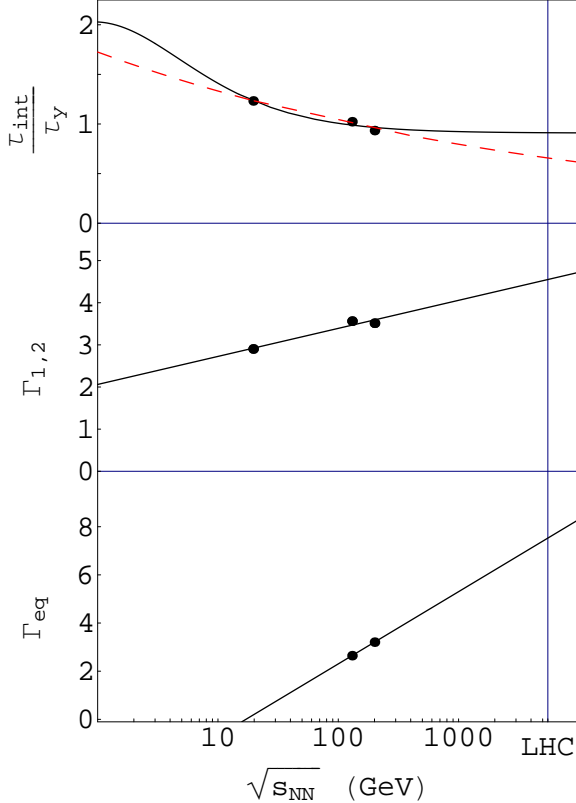


Fig. 1: Dependence of the Diffusion-Model parameters for heavy systems (central Au + Au at RHIC energies) on the center-of-mass energy  $\sqrt{s_{NN}}$ : Quotient of interaction time and relaxation time for sinh- and exponential (dashed) extrapolation (upper frame); width of the peripheral sources including collective expansion (middle frame); effective width of the midrapidity source (lower frame). The results are for charged-hadron rapidity distributions, with extrapolations to LHC energies of 5.52 TeV. The dots refer to the fit values at  $\sqrt{s_{NN}}=19.6, 130$  and 200 GeV.

is performed through the Jacobian

$$J(\eta, \langle m \rangle / \langle p_T \rangle) = \cosh(\eta) \cdot [1 + (\langle m \rangle / \langle p_T \rangle)^2 + \sinh^2(\eta)]^{-1/2}. \quad (5)$$

We approximate the average mass  $\langle m \rangle$  of produced charged hadrons in the central region by the pion mass  $m_\pi$ , and use a mean transverse momentum  $\langle p_T \rangle = 0.4$  GeV/c. Due to the conversion, the partial distribution functions are different from Gaussians.

In the linear two-sources version, the Relativistic Diffusion Model had been applied to pseudorapidity distributions of produced charged hadrons in Au+Au collisions at RHIC energies of 130 GeV and 200 GeV by Biyajima *et al.* [9]. However, it soon turned out from the net-proton results [6], and from general considerations, that an additional midrapidity source is required [6,14]. This source for particle production arises mostly from gluon-gluon collisions and emerges at very short times. In the model we assume that it is generated at  $t=0$  and  $y_{eq}$  with full strength, and then spreads in rapidity space according to Eq.(3) during the strong-interaction time. It comes close to local thermal equilibrium with respect to the variable rapidity during the interaction time  $\tau_{int}$  and hence, we use the notion  $R_{eq}^{loc}(y, t)$  for the associated partial distribution function in  $y$ -space, with  $N_{ch}^{eq}$  charged particles.

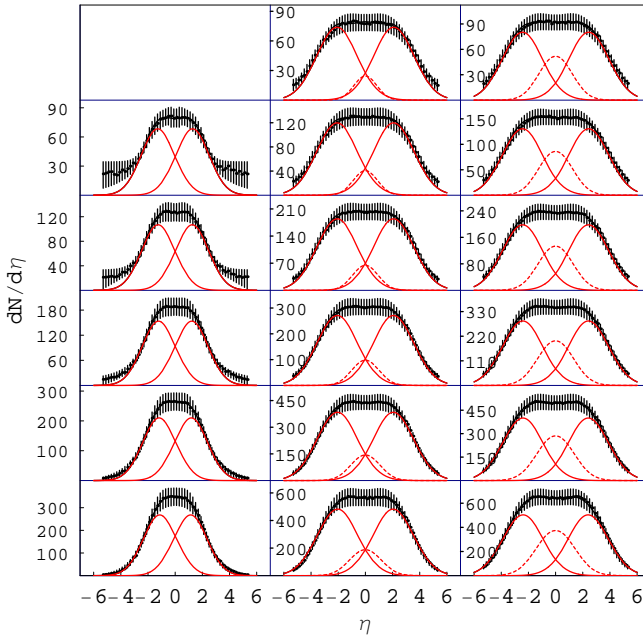


Fig. 2: Calculated pseudorapidity distributions of produced charged particles from Au + Au collisions at  $\sqrt{s_{NN}} = 19.6, 130$  and  $200$  GeV for six collision centralities (sequence as in Figure 3, bottom frames for central collisions) in comparison with PHOBOS data [15]. The analytical RDM-solutions are optimized in a fit to the data. The corresponding  $\chi^2$ -values are given in Table 1. Dashed curves show the midrapidity sources for hadron production.

The validity of this picture was underlined by our recent investigation of the d + Au system at 200 GeV in the three-sources model [10]. Here, an accurate modeling of the gradual approach of the system to thermal equilibrium in rapidity space was obtained. In particular, the dependence of the asymmetric pseudorapidity distribution functions on centrality was precisely described. In the present investigation, however, we concentrate on heavy symmetric systems where QGP formation is more likely.

The dependence of the diffusion-model parameters on incident energy in central Au + Au collisions at RHIC is displayed in Figure 1. Resulting values for the time parameter  $\tau_{int}/\tau_y$  are shown as function of incident energy in the upper frame, with a functional dependence on the absolute value  $y_{max}$  of the beam rapidity and hence, on energy given by

$$\frac{\tau_{int}}{\tau_y} \propto \frac{y_{max} N_{part}}{\sinh(y_{max})} \quad (6)$$

that is discussed in more detail in [17], whereas the dashed curve assumes an exponential dependence on  $\log(\sqrt{s_{NN}})$ . The partial widths as functions of energy within the RHIC range for Au + Au are shown in the middle and lower frames of Figure 1 for both peripheral and midrapidity sources, which differ for produced hadrons. The widths are effective values: beyond the statistical widths that can be calculated from a dissipation-fluctuation theorem, they include the effect of collective expansion. Here we have plotted the values resulting from the  $\chi^2$ -minimization that include the time evolution up to  $\tau_{int}$ , including collective expansion

$$\Gamma_{1,2,eq} = [8 \ln(2) \cdot D_{1,2,eq}^{eff} \cdot \tau_y \cdot (1 - \exp(-2\tau_{int}/\tau_y))]^{1/2}. \quad (7)$$

The charged-particle distribution in rapidity space is obtained as incoherent superposi-

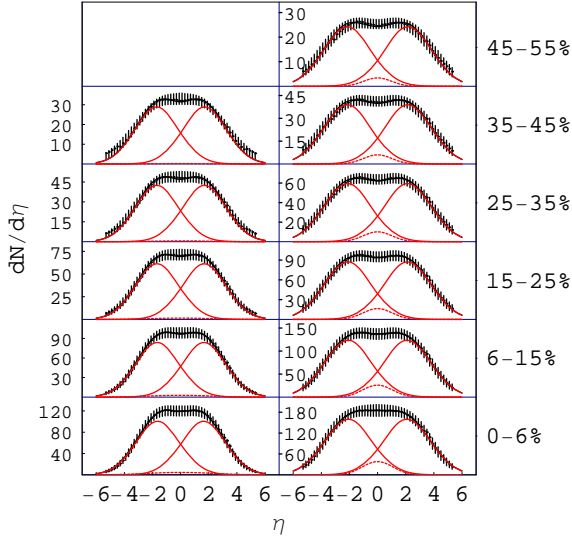


Fig. 3: Pseudorapidity distributions of charged particles from Cu + Cu collisions at  $\sqrt{s_{NN}} = 62.4$  and 200 GeV for six collision centralities in comparison with PHOBOS data [16]. The analytical diffusion-model solutions are optimized in a fit to the data, with constraints discussed in the text. The corresponding  $\chi^2$ -values are given in Table 1.

tion of nonequilibrium and local equilibrium solutions of (3)

$$\begin{aligned} \frac{dN_{ch}(y, t = \tau_{int})}{dy} = & N_{ch}^1 R_1(y, \tau_{int}) \\ & + N_{ch}^2 R_2(y, \tau_{int}) + N_{ch}^{eq} R_{eq}^{loc}(y, \tau_{int}) \end{aligned} \quad (8)$$

with the interaction time  $\tau_{int}$  (total integration time of the differential equation). In the present work,  $\tau_{int}/\tau_y$  is determined together with the set of other free parameters  $\Gamma_{1,2,eq}$  and  $n_{ch}^{eq}$  from the  $\chi^2$ -minimization with respect to the data and hence, the explicit value of  $\tau_{int}$  is not needed as an input. The resulting values for  $\tau_{int}/\tau_y$  are given in Table 1. Although there are rather rapid changes of  $\chi^2$  in narrow intervals of  $\tau_{int}/\tau_y$  due to the simultaneous dependence on the other parameters, the fitting procedure provides a reliable criterion for the determination of the diffusion-model parameters.

**Heavy systems at RHIC.** – Our results for pseudorapidity distributions of produced charged hadrons at six different centralities and three incident energies in Au + Au collisions are shown in Figure 2 in comparison with PHOBOS data [15]. Corresponding results for Cu + Cu at two incident energies are given in Figure 3 compared with preliminary PHOBOS data [16]. At the lowest energy, only two sources are needed for the optimization of the RDM-parameters in a  $\chi^2$ -fit, whereas three sources are indeed required at the higher energies. At the highest energy of 200 GeV, the Cu + Cu system requires a smaller percentage (7%) of particles in the midrapidity source compared to Au + Au, where 26% of the produced hadrons are in the equilibrated source for central collisions. This is consistent with the expectation that heavier systems are more likely to produce a locally equilibrated quark-gluon plasma.

The parameters of these calculations are summarized in Table 1 together with  $\chi^2/d.o.f.$ . The number of degrees of freedom (*d.o.f.*) is the number of data points minus the number of free parameters. We have not aimed at the absolute minimum of  $\chi^2$  as in [9,10] because this does not provide a sufficiently precise determination of the free parameters. Instead, we use physically meaningful constraints to reduce the number of free parameters, and to determine a local minimum.

In particular, we impose a linear decrease of the time parameter  $\tau_{int}/\tau_y$ , of the percentage of particles in the midrapidity source  $n_{ch}^{eq}$ , and of the partial widths  $\Gamma_{1,2,eq}$  with increasing impact parameter. Using these constraints, it is possible to obtain excellent results in the  $\chi^2$ -optimization. Regarding the centrality dependence at fixed incident energy, the increase of the size of the midrapidity source towards more central collisions provides a good reproduction of the data. This is physically reasonable since the midrapidity source is expected to be more important towards more central collisions, where it may originate from an equilibrated parton plasma because of the high energy density.

In a  $\chi^2$ -minimization without any physical constraints [10], the results for the size of the central source as function of centrality have not shown such a trend. Instead the percentage of hadrons in the midrapidity source rises for more peripheral collisions, because the number of charged hadrons produced in the beam-like regions of pseudorapidity space falls more strongly than the overall number of produced particles. In view of the good quality of the constrained centrality dependence in the present work, however, this particular result which is physically difficult to understand may turn out to be an artifact of the fit procedure.

Based on our present calculations at RHIC energies, we have also predicted rapidity distributions of produced charged hadrons in central Pb + Pb collisions at LHC energies using the extrapolations displayed in Figure 1. The results are shown in [17].

**Conclusion.** – To conclude, we have described charged-hadron pseudorapidity distributions in collisions of heavy symmetric systems at four RHIC energies and six centralities with high precision in a three-sources Relativistic Diffusion Model (RDM) for multiparticle interactions. Analytical results for the pseudorapidity distribution of charged hadrons at all investigated centralities are found to be in excellent agreement with the available data. An extrapolation of the transport parameters to LHC energies has been performed.

At the highest RHIC energy of 200 GeV, about 26% of the charged hadrons in central Au + Au collisions are produced in the midrapidity source. These particles come very close to statistical equilibrium in rapidity space during the strong-interaction time. In central collisions with very high energy density, they are likely to originate from a thermalized quark-gluon plasma. The midrapidity source is less pronounced towards more peripheral collisions, lower energies, and in smaller systems such as Cu + Cu. It vanishes at the lowest energy of 19.6 GeV.

## REFERENCES

- [1] WOLSCHIN G., *Eur. Phys. J. A*, **5** (1999) 85; *Europhys. Lett.*, **47** (1999) 30; *Phys. Rev. C*, **69** (2004) 024906.
- [2] KHARZEEV D., LEVIN E. and NARDI M., *Nucl. Phys. A*, **747** (2005) 609; McLERRAN L. and VENUGOPALAN R., *Phys. Rev. D*, **49** (1994) 2233.
- [3] KOIDE T., DENICOL G.S., MOTA P. and KODAMA T., *hep-ph/0609117*, (2006) .
- [4] BRAUN-MUNZINGER P., MAGESTRO D., REDLICH K. and STACHEL J., *Phys. Lett. B*, **518** (2001) 41; ANDRONIC A., BRAUN-MUNZINGER P. and STACHEL J., *Nucl. Phys. A*, **772** (2006) 167.
- [5] BECATTINI F., *Nucl. Phys. A*, **702** (2002) 336.
- [6] WOLSCHIN G., *Phys. Lett. B*, **569** (2003) 67.

- [7] ALBERICO W.M., LAVAGNO A. and QUARATI P., *Eur. Phys. J. C*, **12** (2000) 499; LAVAGNO A., *Physica A*, **305** (2002) 238; ALBERICO W.M., CZERSKI P., LAVAGNO A., NARDI M. and SOMÁ V., *hep-ph/0510271*, (2005) .
- [8] RYBCZYŃSKI M., WŁODARCZYK Z and WILK G., *Nucl. Phys. B (Proc. Suppl.)*, **122** (2003) 325.
- [9] BIYAJIMA M., IDE M., MIZOGUCHI T. and SUZUKI N., *Prog. Theor. Phys.*, **108** (2002) 502; *Prog. Theor. Phys.*, **109** (2003) 151.
- [10] WOLSCHIN G., BIYAJIMA M., MIZOGUCHI T. and SUZUKI, N., *Phys. Lett. B*, **633** (2006) 38; *Annalen Phys.*, **15** (2006) 369.
- [11] TSALLIS C., *J. Stat. Phys.*, **52** (1988) 479.
- [12] UHLENBECK G.E. and ORNSTEIN L.S., *Phys. Rev.*, **36** (1930) 823.
- [13] WOLSCHIN G., *Europhys. Lett.*, **74** (2006) 29.
- [14] BIYAJIMA M., IDE M., KANEYAMA M., MIZOGUCHI T. and SUZUKI N., *Prog. Theor. Phys. Suppl.*, **153** (2004) 344.
- [15] BACK B.B. *et al.*, PHOBOS COLLABORATION, *Phys. Rev. Lett.*, **91** (2003) 052303.
- [16] NOUICER R., PHOBOS COLLABORATION, *private communication*, (2005) ; ROLAND G., PHOBOS COLLABORATION, *Nucl. Phys. A*, **774** (2006) 113.
- [17] KUIPER R. and WOLSCHIN G., *Annalen Phys.*, **16** (2007) 67.